

Development and validation of a dynamic model of the maglev transportation system at Old Dominion University

No. 18

Ajinkyadeodhar, Sebastian Bawab

Department of Mechanical Engineering, Old Dominion University, Norfolk, VA 23508 USA

ajinkyadeodhar@gmail.com, sbawab@odu.edu

Aravind Hanasoge

Department of Aerospace Engineering, Old Dominion University, Norfolk, VA 23508 USA

ahanasog@odu.edu

ABSTRACT: A dynamic model of the vehicle/guideway coupled with a controller is developed for the maglev demonstration system currently being developed at ODU, using the MATHematical DYNAMIC MODELing software - MADYMO. The fundamental characteristics of the vehicle and guideway are obtained from detailed finite element analyses using MSC-NASTRAN. As a result, the vehicle is modeled in MADYMO as a 21-degree-of-freedom spring-mass-damper system. A three span concrete guideway is modeled using 3D solid Hex8 elements. The air gap is modeled as a penetration of the magnets into the guideway. Decentralized co-located PD controllers are used for controlling the penetration of each magnet at steady state levitation. The PD controllers aim at achieving constant penetration (i.e. constant desired air gap) for all magnets.

1 INTRODUCTION

A 12-magnet EMS maglev demonstration system is currently being developed at Old Dominion University (ODU), Norfolk VA campus. As part of this on-going research, finite element (FE) models were developed for the existing vehicle, track and guideway. Dynamic simulation models were also developed to study the vehicle-guideway interaction and the ride quality.

Vehicle-guideway dynamic interaction plays a key role in the overall ride quality of the magnetically levitated and propelled vehicles [2]. Basic analytical results of the vehicle-guideway interaction have been obtained in the past by analyzing the dynamics of one or two mass-spring systems, moving along simply supported Euler-Bernoulli beams [10]. However, as the number of masses increases to more accurately represent the vehicle, the dynamics become complicated and closed form solutions are almost impossible to obtain. This is where a numerical solution using dynamic simulation software becomes very useful. Literature indicates that both vehicle and guideway have been modeled using finite elements [9], [11] and electromagnetic air gaps have been modeled as a penetration [9]. The electromagnetic force to gap relationship has been linearized about a

nominal position, and dynamics of the error around the nominal position has been studied [1], [5], [9]. A typical measure of Ride quality of maglev vehicles has been the Urban Transit Air Cushion Vehicle (UTACV) criterion [8].

In this paper, a dynamic model for the Maglev demonstration vehicle at ODU is developed. This dynamic model is based on the detailed finite element analysis for the vehicle and guideway developed using MSC-NASTRAN. FE dynamic characteristics or modal analysis of the guideway and components of the vehicle such as the bogies have been experimentally verified. Furthermore, a dynamic model is developed using MADYMO [3]. In this regard, the vehicle is modeled as a multi-body spring-mass-damper system, moving along a finite element guideway. The magnetic gap is modeled as a penetration and decentralized PD controllers are used for each magnet. Lateral dynamics of the magnet have not been included in the dynamic model. A numerical simulation is carried out to obtain results of the vehicle ride quality.

The ODU Maglev system as illustrated in Figure 1 is a single vehicle about 13.71 m (45 feet) long, with a capacity to carry 100 passengers, and cover the route of 1.6 km (1 mile) in 3-5 minutes. The total

mass of the vehicle and the chassis assembly together is around 10,890 kg (24,008 lbs). This system uses pulling Electromagnetic Suspension (EMS) technology. EMS maglev systems exhibit inherently unstable dynamics [4] and therefore need feedback control systems to achieve stable levitation.



Figure 1. Maglev at the Old Dominion University, Norfolk Campus

2 MODELING

MSC-NASTRAN was utilized to produce a detailed model of the vehicle as well as the guideway. Modal analyses were conducted to these models in order to validate or capture physical characteristics. The FE model for the basic structure of the body-chassis assembly of the vehicle was developed using 1D CBAR elements and 2D CQUAD elements. Welds were modeled using rigid body elements and bolts using CBAR elements. In the case of the guideway, the model was validated with experimental testing while sections of the vehicle such as the bogies were tested against experiments for validation. These models were utilized in one way or another to build the dynamic model in MADYMO as illustrated in the following sections.

2.1 Modeling of the Guideway

A Bernoulli-Euler beam model is applied to a simply supported, homogenous, isotropic, and uniform cross section guideway. The maximum deflection at the mid span of this beam is given by

$$\delta = \frac{5WL^4}{384EI} \quad (1)$$

Where W is the weight/unit length, E is the bending rigidity and I is moment of inertia about

the bending axis. The characteristics of the ODU guideway are as shown in Table 1.

Property	Value	Unit
Length	27	m
Density	2.409e+03	kg/m ³
Mass	33.803.7e+03	kg
Young's modulus	3.498e+10	N/m ²
Cross section area	0.5203	m ²
Bending moment of inertia	0.0895	m ⁴

The natural frequencies of the guideway model are in close match to the experimental results listed in Table 2. This model is imported from MSC-NASTRAN into MADYMO software without any modifications.

Mode	Euler-Bernoulli Beam	Experimental	NASTRAN FE Model
1 st mode (Hz)	2.82	3.18	2.92
2 nd mode (Hz)	11.71	11.93	11.11
3 rd mode (Hz)	25.43	25.56	23.57

2.2 Modeling of the Magnet in MADYMO

A magnet is modeled as a system combined of a rigid body and finite elements. The magnet is connected to the reference or inertial system with a combination of 2 independent translational joints, for the forward and vertical motions, respectively, as depicted in Figure 2. The Finite elements of the magnet are modeled as zero mass shell elements and are used to determine the penetration (i.e. the air gap). The physical properties of the magnet such as the mass are represented in the rigid body part.

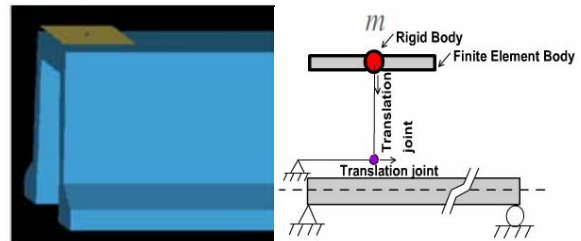


Figure 2. Magnet model comprising of rigid body and finite element body

2.3 Modeling of the Vehicle

The FE model of the vehicle and bogies are depicted in Figures 3 and 4, respectively, and are modeled by a single rigid body as shown in Figure 5. The

positions of the magnets are the same as the physical prototype. The magnetic suspension is modeled by a PD controller equivalence. The suspension that connects the magnet to the bogie, as shown in Figure 5, is modeled by a linear spring-damper system representing the hockey stick flexibility. The magnetic suspension and the hockey stick suspension together constitute the primary stiffness. The bogie to vehicle suspension is modeled using a linear spring-damper and forms the secondary suspension system as shown in Figure 5.

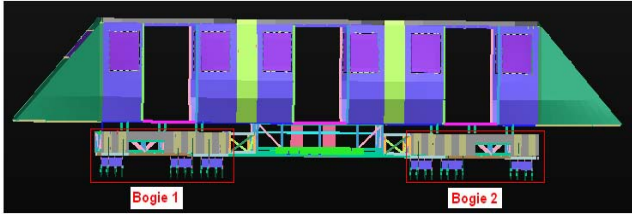


Figure 3. FE model of the Vehicle with 2 bogies

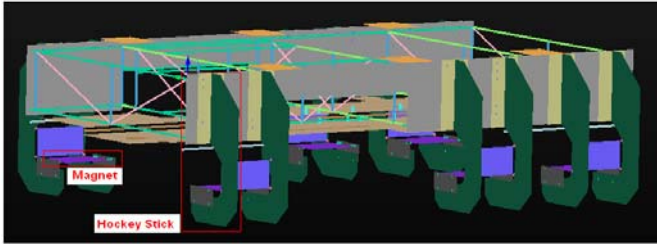


Figure 4. FE model of the Bogie with 6 hockey sticks

The dynamic model of the complete ODU vehicle system as depicted in Figure 6 is modeled as a twenty-one degree of freedom (DOF) three-dimensional (3-D) spring mass system sliding along a finite element guideway.

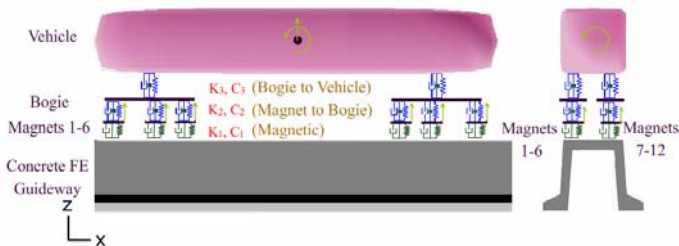


Figure 5. A 21 DOF Dynamic model of ODU system

“ u_1 ” through “ u_{12} ” represent the linear displacement of the 12 magnets along the Z-axis. Both the bogies and the vehicle have 3 degrees of freedom, the heave, the pitch and the roll. Heave is the linear displacement along the global Z-axis, pitch is the rotation about the Y-axis and roll is the rotation along the X-axis. The whole system consisting of the

vehicle, the magnets and the spring-damper is initially levitated and then driven by a constant velocity along the guideway or inertial X-axis.

3 MODELING OF THE PRIMARY SUSPENSION

The primary suspension consists of the magnetic suspension and magnet to bogie (hockey-stick) suspension.

3.1 Magnetic Suspension

In this model, the air gap was modeled as a penetration. The finite element body of the magnet penetrates into the guideway. The penetration is the distance from the top surface of the deflected guideway to the penetrated finite element body of the magnet. To maintain a constant penetration (air gap) between the track and the magnet, the controller is incorporated in the model. The aim of the controller is to determine the magnitude and the direction of the levitation force required to achieve the desired penetration.

The actual electromagnetic force, F is a function of electromagnet physical parameters, the current, I and actual air gap, δ given by Equation 2.

$$F(I, \delta) = \frac{\mu_0 N^2 A}{4} \left(\frac{I}{\delta} \right)^2 \quad (2)$$

Here $\frac{\mu_0 N^2 A}{4}$ is a constant of the magnet equal to $0.002168 \text{ Nm}^2 \text{ A}^{-2}$. μ_0 is the permeability of air, N is the number of turns, and A is the area of contact.

$$I = k_{amps} (\delta - \delta_0) + c_{amps} (\dot{\delta} - \dot{\delta}_0) \quad (3)$$

Where $k_{amps} = 110 \text{ A/in}$ is the stiffness coefficient and $c_{amps} = 1.5 \text{ As/in}$ is the damping coefficient, δ_0 is the desired air gap and $\dot{\delta}$ is the rate of change of air gap (Figure 8).

The values shown above are obtained from experimental real-time testing of the vehicle. The magnetic force is non-linear as shown in Equation 4. It is modeled in MADYMO as a summation of the three forces namely static, stiffness and damping forces.

$$F = F_0 + k(\delta - \delta_0) + c(\dot{\delta} - \dot{\delta}_0) \quad (4)$$

Where F is the total magnetic force, F_0 is the static magnetic force or weight, $k(\delta - \delta_0)$ is the stiffness force, $c(\dot{\delta} - \dot{\delta}_0)$ is the damping force. To compute the total force F , in Newton units, it is required to convert the k_{amps} and c_{amps} into N/m and Ns/m, respectively.

$$F_{stiffness} = \frac{\mu_0 N^2 A}{4} k_{amps}^2 \frac{(\delta - \delta_0)^2}{\delta^2} = k(\delta - \delta_0) \quad (5)$$

The above equation shows that the stiffness, k in N/m varies with the actual air gap δ and desired air gap δ_0 . The stiffness force is a non-linear function of air gap as shown in Figure 6. The force is zero when the desired air gap of 0.00762 m is achieved.

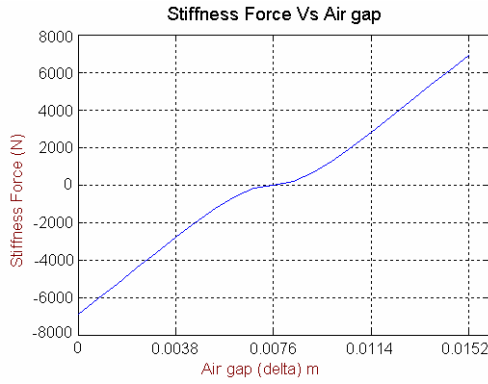


Figure 6. Stiffness Force vs. Air gap

Similarly,

$$F_{damping} = \frac{\mu_0 N^2 A}{4} c_{amps}^2 \frac{(\dot{\delta} - \dot{\delta}_0)^2}{\delta^2} = c(\dot{\delta} - \dot{\delta}_0) \quad (6)$$

The above equation shows that the damping, c in Ns/m varies with the actual rate of change of air gap, $\dot{\delta}$ and desired rate of change of air gap $\dot{\delta}_0$. The damping force is a non-linear function of rate of change of error in air gap as shown in Figure 7. The CONTACT element of MADYMO is used in modeling the levitation force. Sensors determine the location and velocity at every time step of the simulation. Penetration and velocity of the penetration are determined and the control feedback system is represented as shown in Figure 9.

From Equation (4), the PD controller force is given by

$$F = k(\delta - \delta_0) + c(\dot{\delta} - \dot{\delta}_0) \quad (7)$$

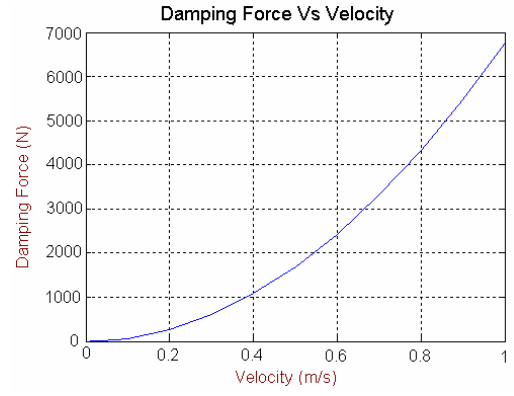


Figure 7. Damping Force Vs Rate of change of error in gap

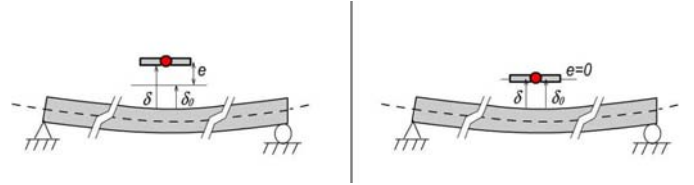
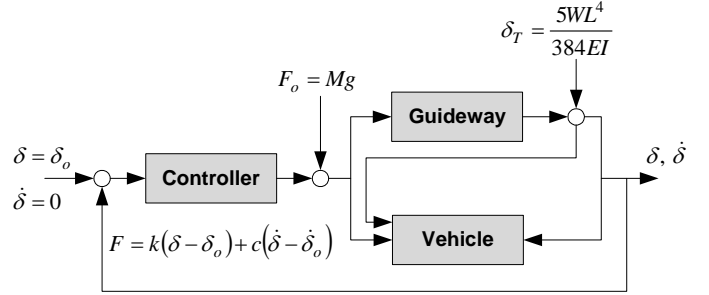


Figure 8. Symbolic representations of the error δ



- | | |
|---|-------------------------------------|
| δ = Actual Magnetic gap | δ_r = Deflection of guideway |
| $\dot{\delta}$ = Rate of change of error in gap | W = Guideway weight |
| δ_0 = Desired Magnetic gap | L = Guideway length |
| K = Proportional gain | EI = Guideway rigidity |
| C = Derivative gain | x = Vehicle position |
| F_0 = Vehicle weight | F = Control force |

Figure 9. System configuration

The sensor δ measures the penetration of the magnet (i.e. the air gap) and the sensor $\dot{\delta}$ measures the rate of change penetration. As shown in Figure 9, the value of these 2 sensors is compared with the desired set point values where $\delta = \delta_0$ and $\dot{\delta} = 0$. If the set point conditions are satisfied, the coefficients of k and c in the controller force given by Equation (7) become zero, hence the total controller force is null. But the force F_0 due to vehicle weight is applied to the guideway. Whereas if the set point conditions are not satisfied, the controller force is determined according to Equation (7).

The total dynamic force given by Equation (4) acts on the magnet in the upward direction and equal

and opposite force is acted on the guideway. As a result of the dynamic force, the guideway deflects and changes the gap. In the next time step, the feedback of the two sensors determines the gap error, which in turn determines the magnitude of controller force required to achieve the desired gap.

3.2 Magnet to Bogie Suspension

The vertical edges of the hockey stick are fixed and the modal frequency analysis is performed using MSC-NASTRAN. The magnets frequency in the vertical direction in Mode 3 is 95.47 Hz. The corresponding structural stiffness is $k_s=3.23e+07$ N/m and structural damping is $c_s=2.692e+03$ Ns/m.

4 MODELING OF SECONDARY SUSPENSION

The secondary suspension consists of the connection between the bogie and the vehicle center of gravity. In the MSC-NASTRAN finite element model, the node at the center of each magnet is fixed in the vertical direction and connected to the ground by a spring element. This model simulates the conditions of the levitated vehicle. The roll, pitch and heave frequencies are recorded as 1.96 Hz, 4.35 Hz, and 4.72 Hz, respectively, to create K_3 and C_3 values.

A similar model to the above mentioned MSC-NASTRAN model is developed in MADYMO by connecting the magnets to the ground using the springs. In the MADYMO model, the stiffness of the springs connecting the bogies to the vehicle as seen in Figure 5 is selected such that the Roll, Pitch and Heave frequencies of the vehicle are similar. The stiffness of the 4 springs in the vertical direction is given as follows. Accordingly, the left front and right front spring stiffness values are $2.353e+06$ N/m and $2.359e+06$ N/m, respectively, and the rear left and rear right springs are $1.637e+06$ N/m and $1.629e+06$ N/m, respectively. In addition, there is a lateral stiffness for each magnet equal to $1.179 +06$ N/m.

Based on these stiffness values and assuming a damping ratio of 0.025 for all suspension points, the MADYMO model produced a roll frequency of 1.74 Hz, while the pitch frequency is 4.98 Hz and the heave frequency is 4.13 Hz. These values closely match the MSC-NASTRAN results.

5 ODU MAGLEV TRAVELLING AT SPEED OF 20m/s

The maglev with the non-linear magnetic stiffness and damping is levitated in the middle of the vertical support or pillar, as shown in Figure 10.

Once the vehicle achieves a steady state levitation, its speed is ramped up to a constant velocity 20 m/s (45 mph) for which the ODU maglev system is designed.

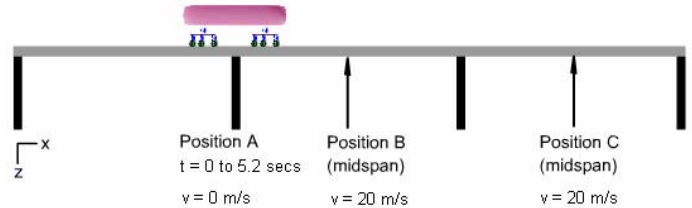


Figure 10. Vehicle locations

The actual air gap is as shown in Figure 11. The vehicle vertical acceleration is below the Advanced Ground Transportation AGT [5] limit of 0.05g ($.49$ m/s^2) as shown in Figure 12.

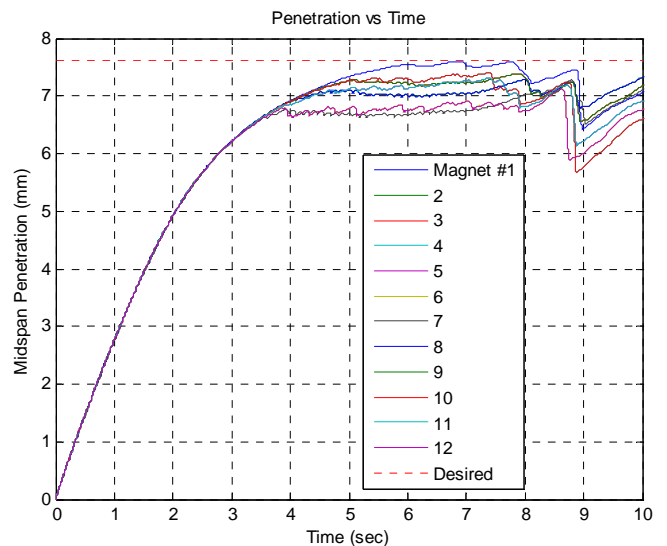


Figure 11. Actual air gap of 12 magnets

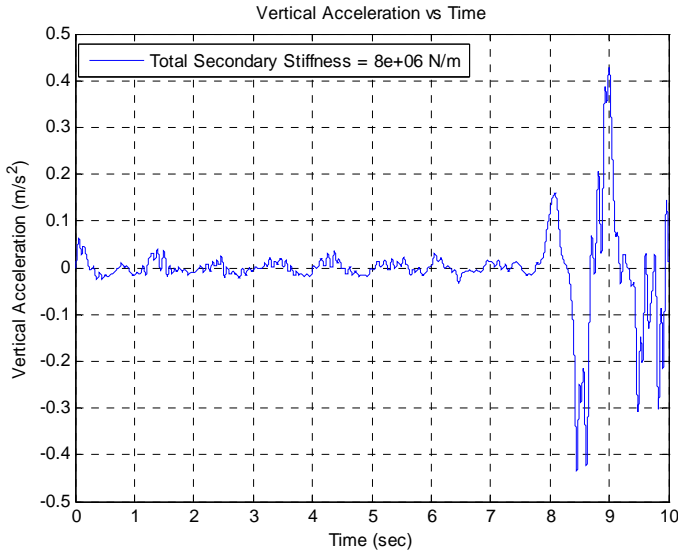


Figure 12. Vehicle vertical acceleration vs. Time

The mid-span deflections of the 2nd and 3rd span of the guideway are about 11 mm and 10.5 mm, respectively, as shown in Figure 13. As the guideway is supported by a roller at the 2nd and the 3rd span, the direction of displacement (slope) of the mid-span of 2nd and 3rd span is opposite in nature.

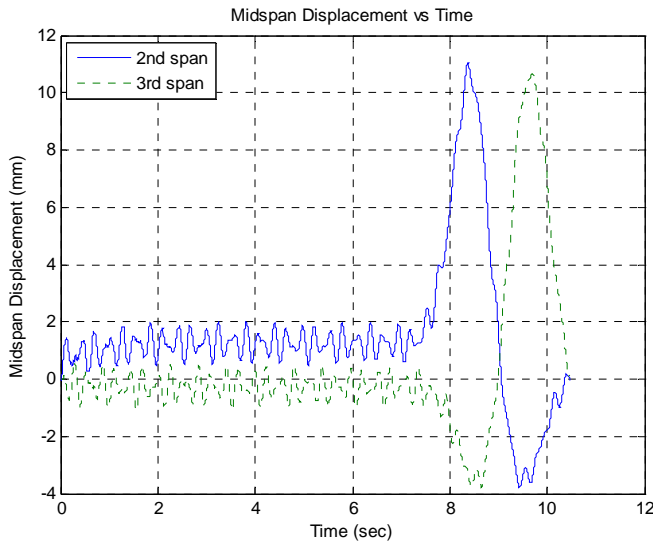


Figure 13. Mid-span displacement vs. Time

6 UTACV RIDE QUALITY

The US Department of Transportation has proposed a guideline for Advanced Ground Transportation (AGT) systems in 1971, which is known as UTACV (the Urban Tracked Aircushion Vehicle) criterion as shown in Figure 14 [5]. This ride quality criterion is

widely used to evaluate dynamic behavior of high speed transportation systems. Also the allowable limit for the vertical acceleration is 0.05g, which is 0.4905 m/s².

The maximum vertical acceleration of the ODU system is less than 0.4905 m/s² as shown in Figure 13. But the PSD of the vehicle vertical acceleration does not meet the UTACV ride quality criterion as shown in Figure 16. It is seen that for the 27 meter span length of the ODU guideway, a 1 Hz periodic response appears in the PSD curve for the vehicle travelling at 20 m/s (45 mph) due to interaction with the rigid piers.

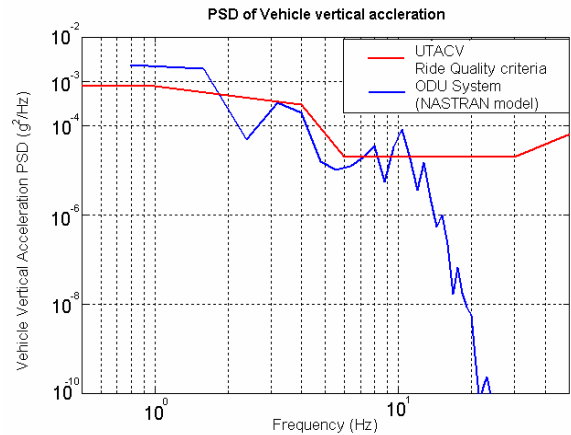


Figure 14. PSD of vehicle vertical acceleration of ODU system

7 CONCLUSIONS

A 21 degree-of-freedom real-time dynamic model for ODU Maglev system is developed to simulate the dynamic interaction between the vehicle and the guideway. The frequency and mid-span deflection of the guideway model in MADYMO is validated with the experimental and Modal analysis (MSC-NASTRAN) results for the guideway. The heave, pitch and roll frequencies of the vehicle in MADYMO model is validated with the FE analysis frequencies obtained from MSC-NASTRAN model.

The magnetic force is linearized in almost all the previous simulations conducted in this area. Based on the physical characteristics of the ODU system, the magnetic force is modeled as a non-linear function of air gap in this MADYMO model. The PD controller works best at steady state and induces error in the transient region of the vehicle levitation.

This validated MADYMO model is then used to study the ride quality of the ODU system for a perfectly flat surface guideway. The maximum acceleration of the vehicle is below the specified

limit of 0.05g (.49 m/s²). But the PSD of the vehicle acceleration traveling at a desired speed of 20 m/s (45 mph) does not meet the UTACV criterion. Further study needs to be pursued to evaluate the affect of a passive secondary suspension system to the vehicle ride quality.

ACKNOWLEDGMENTS

The authors express sincere thanks to the entire Maglev team at Old Dominion University for the continuous inputs in modeling and validation of this dynamic model.

REFERENCES

- [1] Cai, Y., Chen, S. S., Rote, D. M. and Coffey, H. T.. 1996. Vehicle/guideway dynamic interaction in maglev systems, *ASME Journal of Dynamic Systems, Measurement, and Control*, Vol. 118, September 1996, pp. 526-530
- [2] Hanasoge A.M., Hans S.A., Desetty S., Hou, G. J, Alberts T E. 2005. Effects of Track Irregularities on dynamic responses of a moving Maglev train, SAE Conf. paper 2005-01-0504.
- [3] TNO MADYMO 6.2 2004. Theory Manual, TNO Automotive, Delft, Netherlands,
- [4] Sinha, P.K., *Electromagnetic Suspension, Dynamics and Control*, Peter Peregrinus Ltd., London, U.K.
- [5] Zhao, C.F. and Zhai, W.M. 2002. Maglev vehicle/guideway vertical random response and ride quality, *Vehicle System Dynamics*, Vol. 38, No.3, pp. 185-210
- [6] MSC NASTRAN Version 2006, MSC Corporation, USA,
- [7] TNO MADYMO 6.2 Reference Manual. 2004. TNO Automotive, Delft, Netherlands.
- [8] Anon. 1972. *Specification for Urban Tracked Air Cushion Vehicle* (UTACV). DOT U.S., Washington D.C.
- [9] Hyung, S.H., Young, J.K., Byung, C.S., Byung, H.K., Kimm, D. 2006. Simulation of Dynamic Interaction between Maglev and Guideway using FEM, *Maglev 2006 Conference*, 2006.
- [10] Cai, Y., Chen, S. S., Rote, D. M. and Coffey, H. T. 1994. Vehicle/Guideway Interaction for High Speed Vehicles on a Flexible Guideway, *Journal of Sound and Vibrations*, Vol. 175(5), pp. 625-646
- [11] Shi, J., Wei, Q. and Zhao, Z. 2007. Analysis of dynamic response of the high-speed EMS maglev vehicle/guideway coupling system with random irregularity, *Vehicle System Dynamics*, Vol. 45, No. 12, December 2007, pp. 1077-1095